Physics and Imaging in Radiation Oncology 6 (2018) 83–88

Contents lists available at ScienceDirect

Physics and Imaging in Radiation Oncology

journal homepage: www.elsevier.com/locate/phro

Original Research Article

Optimizing radiosurgery with photons for ocular melanoma

I. Frank Ciernik[a,b,*], Markus Wösle[a], Lothar Krause[c], Jérôme Krayenbuehl[d]

[a] Department of Radiotherapy and Radiation Oncology, Dessau City Hospital, Dessau, Germany
[b] University of Zürich, Zürich, Switzerland
[c] Department of Ophthalmology, Dessau City Hospital, Dessau, Germany
[d] Department of Radiation Oncology, University Hospital, Zürich, Switzerland

ARTICLE INFO

Keywords:
Melanoma
Uveal melanoma
Choroidal melanoma
Ocular melanoma
Stereotactic
Radiosurgery
SBRT
IMRT
VMAT
HybridArc
Automated planning

ABSTRACT

Background and purpose: Photon radiotherapy has been established for the treatment of ocular melanoma (OM). Here we investigate the planning qualities of two different planning approaches, a combination of dynamic conformal arcs (DCA) complemented with multiple non-coplanar static intensity-modulated (IMRT) fields (DCA-IMRT), and volumetric modulated arc therapy (VMAT) in combination with automated planning (AP).

Materials and methods: Thirteen consecutive patients treated for ocular melanoma with curative intent on a Linac-based radiosurgery system were analyzed. Fractionated stereotactic radiosurgery (fSRS) was applied using 50 Gy in 5 fractions using the combination of DCA-IMRT. Plans were reviewed and the thirteen cases were compared to plans obtained with optimized automated VMAT based on a set of 28 distinct patients treated with DCA-IMRT who were selected to generate the AP model for the prediction of dose volume constraints.

Results: Overall, plan quality of DCA-IMRT was superior to AP with VMAT. PTV coverage did not exceed 107% in any case treated with DCA-IMRT, compared to seven patients with VMAT. The median PTV covered by > 95% was 98.3% (91.9%–99.7%) with DCA-IMRT, compared to 95.1% (91.5%–97.9%) ($p < 0.01$) with VMAT. The median mean dose delivered to the treated eye was 22.4 Gy (12.3 Gy–33.3 Gy) with DCA-IMRT compared to 27.2 Gy (15.5 Gy–33.7 Gy) ($p < 0.01$). Dose to the ipsilateral lacrimal gland and the ipsilateral optic nerve were comparable for DCA-IMRT and VMAT, however, the dose to the lens was lower with DCA-IMRT compared to VMAT.

Conclusions: The combination of multiple arcs complemented with multiple IMRT fields sets the gold standard for fSRS of ocular melanoma for photon therapy.

1. Introduction

Linac-based radiosurgery with photons has been investigated and applied for more than twenty years [1,2]. Classical radiosurgery of ocular melanoma (OM) uses multiple conformal arcs with multi-leaf collimators prescribing to the 80% isodose line [1]. Photons have been shown to achieve adequate target coverage for treating ocular melanoma compared to protons [3,4], and acceptable to excellent clinical results have been reported for Linac-based radiosurgery [5–7]. The challenge with photons relies in achieving steep dose gradients avoiding unnecessary dose to neighbouring structures. Eye positioning for photon therapy is more complex as compared to proton therapy due to variable beam angles used. Approaches with open eye gaze fixation or forced fixation with suction-based devices may rule out specific beam field geometries and thus limit the degree of freedom to optimize the dose distribution. The most patient-convenient approach is to have the patient positioned with eyes closed without any need of medication or specific interventions, and a X-ray based positioning verification system based on tissue markers surrounding the tumor and target structure and treating patients with their eyes closed has been proposed previously [8].

Volumetric modulated arc therapy (VMAT) has been increasingly promoted in radiosurgery during the last years mostly because it can treat multiple lesions with one isocenter [9,10]. However, the combination of non-coplanar arcs with IMRT improves dose coverage and homogeneity, because it allows steep dose fall-offs by adding static IMRT [11]. Here we investigate, whether automated planning with multiple, non-coplanar modulated arcs, known as VMAT or IMAT (intensity modulated arc therapy) could result in treatment plans comparable to the quality of plans with DCA-IMRT.

2. Materials and methods

2.1. Patients

For this retrospective treatment planning comparison, patients

* Corresponding author at: Strahlentherapie und Radioonkologie, Städtisches Klinikum Dessau, Auenweg 38, 06846 Dessau, Germany.
E-mail addresses: ilja.ciernik@klinikum-dessau.de, ilja.ciernik@uzh.ch (I.F. Ciernik).

https://doi.org/10.1016/j.phro.2018.06.001
Received 14 August 2017; Received in revised form 26 May 2018; Accepted 1 June 2018

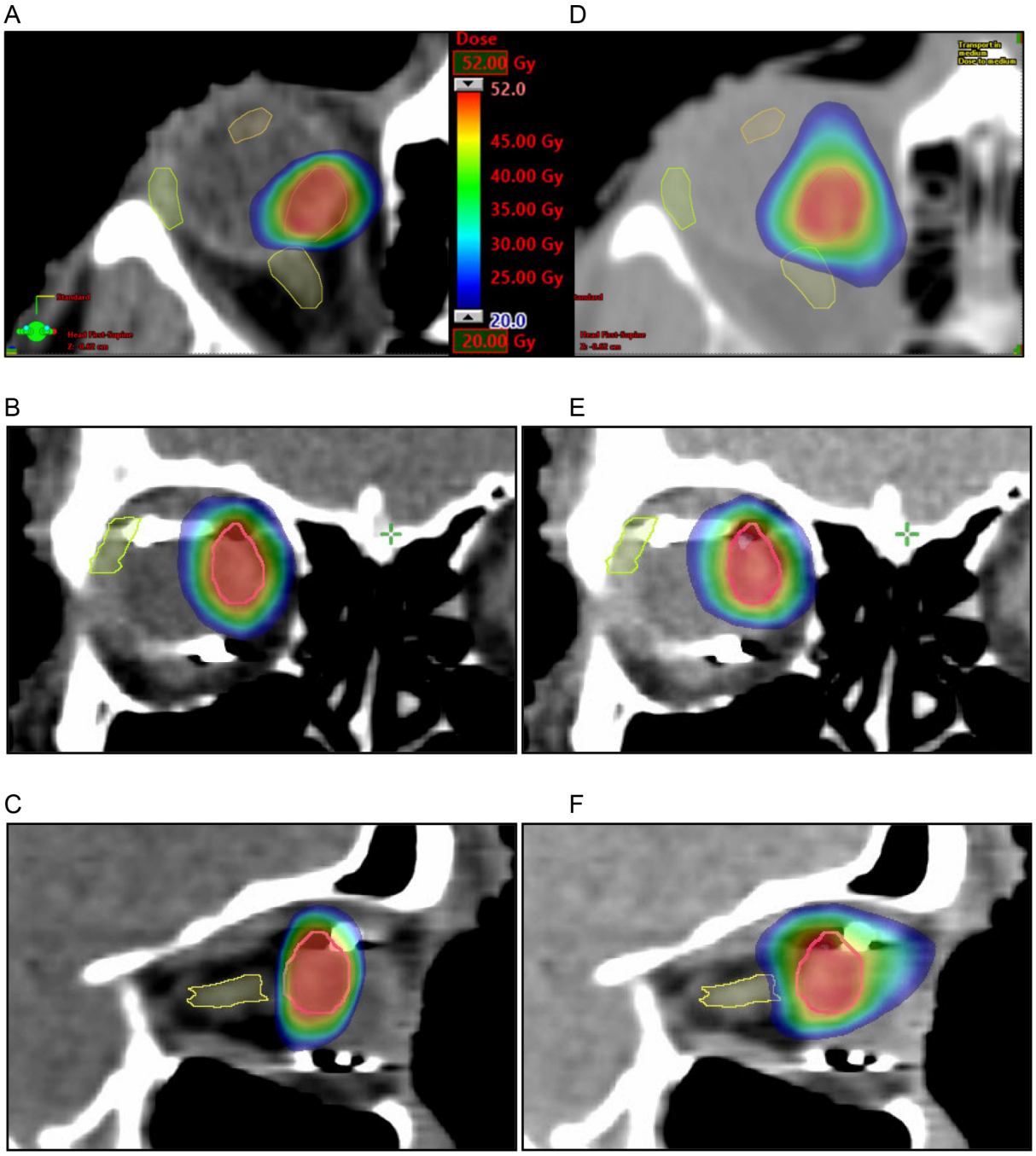

Fig. 1. Isodoses of DCA-IMRT (a,b,c) and VMAT (d,e,f) of a representative case. Axial (a and d), coronal (b and e), and sagittal planes (c and f). Scale as in Fig. 1a applies to all images, showing dose ranging from 20 to 52 Gy.

treated between 2014 and 2016 for curative radiotherapy of ocular, non-metastatic melanoma were enrolled. Patients were treated with a dose fractionation of 5 × 10 Gy on five consecutive days. All patients included into this study have given their approval to use their data for scientific research, and all were treated with the Hybrid-Arc™ technique. Prior to radiotherapy planning, three ophthalmological tantalum markers (Altomed Ltd., Boldon, UK) were attached on the sclera surrounding the tumor. A fourth marker was sutured to the opposite half of the bulb. Magnetic resonance imaging (MRI) and a planning computer tomography (CT) were obtained and fused images served for target volume definition. The gross tumor volume (GTV) was outlined on the MRI obtained after placement of the peritumoral fiducial markers and verified on the CT images. The margins to obtain the planning target volume (PTV) were two mm in general and occasionally three mm in the direction of the vitreous body or in direction of retinal detachment.

The treated plans for DCA-IMRT were manually optimized for a photon linear accelerator (Novalis-TrueBeam™; BrainLab and Varian Medical Systems) with a dynamic high-definition multi-leaf collimator. The dose was normalized to the mean value of the PTV. Clinically accepted and delivered treatment plans served as reference in this study. All treatment plans were verified with the physician before treatment. During treatment image-guidance by means of the ExacTrac™ 6.0.6 and Robotics® 2.0. (BrainLab, Feldkirchen, Germany) was used, positioning was verified prior to each beam or arc fraction. Tantalum markers were used for the positioning verification. The daily energy dose fractions of flattening filter free (FFF) 5.6 MeV photons were delivered by the frameless BrainLab® radiosurgery system.

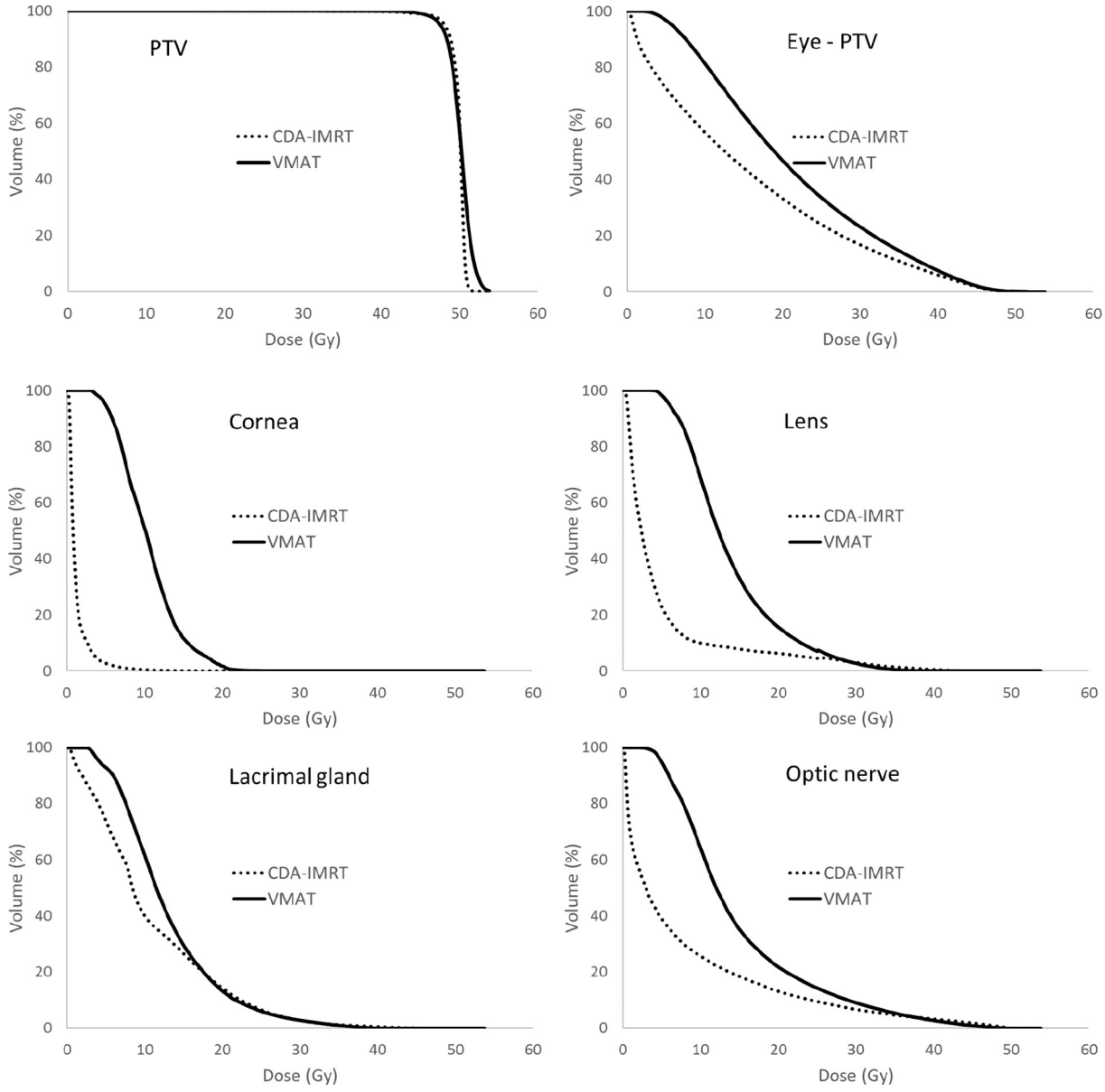

Fig. 2. Average dose volume histograms of 13 plans calculated with DCA-IMRT (dotted line) or VMAT (solid line). (a) PTV, (b) Eye without PTV, (c) ipsilateral cornea, (d) ipsilateral lens, (e) ipsilateral lacrimal gland, and (f) ipsilateral optic nerve.

2.2. Planning of multiple conformal arcs with IMRT and beam geometry

All patient treated for ocular non-metastatic melanoma were planned to be treated with DCA-IMRT by the module HybridArc™ (HA) of the treatment planning system iPlan® RT Dose 4.5.3 and 4.5.4 (BrainLab AG, Feldkirchen, Germany). On average, a combination of six dynamic conformal arcs, ranging from five to six, with six intensity-modulated static fields, ranging from five to eight, were used. A single isocenter for each plan was used. The beam arrangement was set in such a way that no beam went through the ipsilateral cornea or the contralateral eye. The geometry of the non-coplanar dynamic conformal arcs was manually optimized. The arc lengths ranged from 30° to 110° and the couch kick angle increments ranged from 15° to 60°. The dose contribution of the arcs to the target was approximately 70% of the prescribed dose. Subsequently, IMRT fields delivered the remaining 30% of the prescribed dose. The couch angles used for the IMRT fields were the same as those used for the dynamic conformal arcs. Thus the additional IMRT fields could be delivered “on the way” without waste of time. The IMRT fields were optimized with a maximum beamlet size of 2.0 mm in dynamic leaf sequencing. The dose calculation algorithm used was BrainLAB PencilBeam X, using a kernel resolution of 0.63 mm. One effective parameter to find a good compromise on coverage of planning target volume and sparing of organs at risk (OARs) is the percentage of IMRT dose; this value ranged from 27 to 36%.

2.3. Planning with VMAT

The plan optimization with VMAT was automated using RapidPlan™ (RP) (Varian Inc., Palo Alto, USA) with the photon optimizer version 13.6.23 and Acuros version 13.6.23 as algorithm for dose calculation. RP is a fully integrated module in the treatment planning system Eclipse, similar to the “manual” inverse optimizer module and has been previously explained [12]. Briefly, RP automates the optimization process by generating a line of objectives constraints based on the geometry of the PTV and OARs. The objectives are set just below the inferior boundary of the predicted result. Therefore the plans generated with RP are independent from the planner knowledge and the results are, in general, at least as good or better than the plans manually

optimized [12,13].

The model generated for the present study was built in a similar way as for the other validated and clinically implemented models used for disease of the brain, lung and prostate. The model created in RP was generated from 28 irradiated patients treated with DCA-IMRT, distinct from the thirteen cases used for the planning comparison, who were not included in the model in order to avoid a bias of the results. Plans optimized with RP were not included in the model. The optimization constraints used for each OARs consisted on a line of DVH objectives as well as a maximum allowed dose. These constraints were automatically generated by the system based on the predicted achievable dose distribution from the RP model. The constraints and objectives for the PTV, were predefined in the RP model. The lower and upper constraints were set between 150 and 200. The contralateral eye was given a priority of 50. The ipsilateral eye and cornea was given a maximal dose with a priority of 70 to 90. The dose to the ipsilateral lacrimal gland for D20 Gy was set at a priority of 50–70. The priority for the Dmax for the ipsilateral lens and optic nerve was set at 90–120.

All patients were planned with VMAT for Linac TrueBeam™ (Varian Inc., Palo Alto, USA), having the same specification as the one used for the optimization and treatment with HA. Six arcs with three to five couch kicks were used. The angle separation between the different couch positions was at least fifteen degrees. The beam geometry was manually set case by case in order minimize the entrance dose through an OAR. Density compensation for tantalum tissue marker density was not applied.

2.4. Plan comparison

The treatment calculation grid size for DCA-IMRT and VMAT was 1 mm for voxels within the PTV, and never exceeded 1.5 mm at opposite site of the tumor in the eye. The linac used in both institutions had similar specification (TrueBeam and Novalis STx have both a HDMLC) and the same beam energy was used (6MV). Dose volume histograms (DVHs) were calculated for the PTV and OARs of each plan. As OARs, we scored cornea, lens, lacrimal gland, optic nerve, and the entire eye, and the entire eye without the PTV. For comparison purposes, DVHs were normalized to the mean dose of the PTV (50 Gy over five fractions). Target dose distribution was evaluated according to the target coverage defined as the volume enclosed by the 95% and 107% isodose line, $V_{95\%}$ or $V_{107\%}$, respectively, and dose to the critical structures, such as lenses, cornea, lacrimal glands and optic nerves were analyzed. Dose homogeneity was defined by the homogeneity index (HI) defined as $HI = (D_{5\%} - D_{95\%})/Dmean$, where $D_{5\%}$ and $D_{95\%}$, are the dose to 5% or 95%, respectively of the target and D_{mean} is the mean dose to the target [14]. The conformity index (CI) was defined as $CI = 1 + [V_{95\%}(NT) - V_{95\%}(PTV)]/V(PTV)$, where $V_{95\%}$ (NT) is the normal tissue volume covered by the 95% prescribed dose, $V_{95\%}$ (PTV) is the target volume covered by 95% of the prescribed dose and V(PTV) is the target volume [15]. Statistical analysis was performed using a Wilcoxon test. A p-value of < 0.05 was accepted as significant.

The dose to the OARs was evaluated accordingly to the mean dose for all OARs, the maximal dose defined as the dose to a volume of 0.03 cm^3, $D_{0.03cm3}$. For the ipsilateral lacrimal gland, an addition parameter was used, the volume receiving 20 Gy, V_{20Gy}.

An evaluation of the robustness in respect to a motion of the eye was performed. The robustness of the plan was evaluated based on the target volume covered by the 95% prescribed dose, $V_{95\%}$. A simulation of an eye motion resulting in a translation of the target by 2 mm in each direction: left-right, cranial-caudal and ventral-dorsal was performed. The isocenter remained at the same location, only the target was shifted in a single direction at one moment. This simulation was performed for five right-sided cases.

3. Results

3.1. Clinical aspects

Since December 2014 until August 2016, 28 consecutive patients with a mean age of 68 years with ocular melanoma were treated with fractionated radiosurgery on 5 consecutive working days with 5 × 10 Gy and served as model to establish automated planning with VMAT. After a median follow-up of seventeen months, no local relapse was observed. Enucleation was necessary in one patient due to erosive keratitis 31 months after the end of radiotherapy. Metastatic progression to the liver was seen in two patients. In one case, 20 months after radiotherapy metastatic liver disease was observed. Another patient suffered metastasis to the liver fifteen months after DCA-IMRT and was treated with hemihepatectomy. He died from postoperative infection at the age of 87 years.

3.2. PTV coverage

Beam geometries for DCA-IMRT were 5–6 dynamic conformal arcs and 5 to 8 IMRT fields. VMAT plans used 6 arcs for each case. The quality of the PTV coverage was defined by the comparison of 13 cases recalculated with VMAT and plans optimized with RP. The isodose map in axial coronal, and sagittal planes shows steeper dose fall off with DCA-IMRT compared with VMAT (Fig. 1). The average dose volume histogram is shown in Fig. 2a, showing that the target volume coverage achieved with DCA-IMRT and VMAT was similar under ICRU-criteria. Minor qualitative differences were detected. Dose exceeding 107% in 7 patients (54%) replanned with VMAT was observed. The homogeneity index (HI) for the PTV was 0.06 ranging from 0.01 to 0.13 for DCA-IMRT and 0.1 ranging from 0.05 to 0.12 for VMAT, respectively ($p < 0.01$). The conformity index for DCA-IMRT was 1.24 (1.05–1.77) and 1.31 (1.11–1.50) for VMAT ($p = 0.25$). The robustness of plans with DCA-IMRT and VMAT was analyzed for the first five right-sided cases. It was based on the effect of a target motion in one direction on the $V_{95\%}$. VMAT gave significant better results than DCA-IMRT when a target motion would occur in the lateral with a median $V_{95\%}$ of 88.4% (83.5%–90.4%) vs. 81.4% (78.4%–84.9%), in caudal, 90.3% (85.7%–94.0%) vs. 85.0% (78.5%–86.3%) or dorsal direction, 89.2% (86.4%–91.5%) vs. 85.1% (79.5%–86.0%) direction ($p < 0.01$) by 2 mm. The median average $V_{95\%}$ after target displacement was 83.3% (81.3%–86.2%) ± 3.4% for DCA-IMRT and 87.4% (83.5%–90.6%) for VMAT ($p < 0.01$) (Fig. 3).

3.3. Organs at risk

DCA-IMRT and VMAT were compared regarding dose delivered to

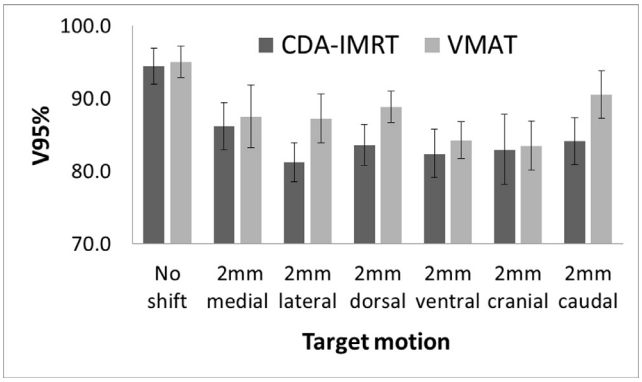

Fig. 3. Analysis of robustness for DCA-IMRT and VMAT. Shift in 6 directions was analyzed. Significant differences were noticed in lateral, caudal, and dorsal direction ($p < 0.05$).

Table 1
Dose volume histogram parameters: comparison of DCA-IMRT and VMAT.

		DCA-IMRT		VMAT		*p*-value
		median	range	median	range	
PTV	V95 (%)	98.3*	91.9–99.7	95.1	91.5–97.9	< 0.01
	V107 (%)	0*	0–0	0.2	0–1.2	< 0.01
	HI	0.05*	0.01–0.13	0.1	0.05–0.12	< 0.01
	CI	1.24	1.05–1.77	1.31	1.11–1.50	0.3
Ipsilateral optic nerve	D 0.03 (Gy)	28.1	18–49	31.1	16.2–46.8	0.2
	Mean dose (Gy)	7.3*	0.4–22.2	13.4	8.2–17.4	< 0.01
Contralateral optic nerve	D 0.03 (Gy)	0.2*	0.1–4.1	1.7	0.8–2.9	< 0.01
	Mean dose (Gy)	0.1*	0.1–2.1	1.6	0.6–2.5	< 0.01
Ipsilateral lens	D 0.03 (Gy)	5.5*	1–37.2	17.0	9.0	33.3
	Mean dose (Gy)	3.7*	0.6–26.8	13.3	4.1–25.4	< 0.01
Contralateral lens	D 0.03 (Gy)	0.1*	0.1–0.3	1.3	0.2–2	< 0.01
Ipsilateral lacrymal gland	D 0.03 (Gy)	24.6	4.4–38.5	22.0	5.4–39.3	0.3
	Mean dose (Gy)	12.5*	1.7–21.4	14.0	3.9–22.9	0.04
	V20Gy (%)	14.0	0–57.6	11.4	0–62.1	0.2
Contra. lacrymal gland	Mean dose (Gy)	0.1*	0.1–0.2	0.8	0–1.4	< 0.01
Ipsilateral eye	Mean dose (Gy)	22.4*	12.3–33-3	27.2	15.5–33.7	< 0.01
Contralateral eye	Mean dose (Gy)	0.1*	0.1–0.2	1.4	0.2–1.6	< 0.01

Abbreviations: DCA-IMRT: dynamic conformal arcs combined with multiple non-coplanar static intensity-modulated radiotherapy; VMAT = volumetric modulated arc therapy; PTV = planning target volume; $V_{107\%}$ = volume receiving a dose of 107% or more; $D_{0.03cm}{}^{3}$ = dose to 0.03 cm^3 of the respective organ. * Significance ($p < 0.05$).
HI: Homogeneity index; CI conformity index.

neighbouring structures. Treatment was feasible within clinical acceptable limits for DCA-IMRT and VMAT, although better dose sparing was achieved with DCA-IMRT (Table 1). With DCA-IMRT, dose to the contralateral eye was avoided, leaving dose only from scattered photons. The dose to the contralateral eye was 0.1 Gy (0.1 Gy–0.3 Gy) for DCA-IMRT and 1.4 Gy (0.2 Gy–1.6 Gy) for VMAT ($p < 0.01$). The dose delivered to the ipsilateral eye was greater for VMAT than for DCA-IMRT. On average, the dose given to the affected eye excluding the target volume was 22.4 Gy (12.3 Gy–33.3 Gy) with DCA-IMRT and 27.2 Gy (15.5 Gy–33.7 Gy) for VMAT ($p < 0.01$) (Table 1 and Fig. 2b). In the anterior direction, the dose values given to the cornea and lens were higher with VMAT as compared with DCA-IMRT. The mean dose to the lens with DCA-IMRT was 3.7 Gy (0.6 Gy–26.8 Gy) compared to 13.3 Gy (4.1 Gy–25.4 Gy) for VMAT (Table 1 and Fig. 2d) ($p < 0.01$). The doses delivered to the lacrimal gland were improved with DCA-IMRT, with a median mean dose of 12.5 Gy (1.7 Gy–21.4 Gy) compared to 14.0 Gy (3.9 Gy–22.9 Gy) with VMAT ($p = 0.04$), respectively (Table 1 and Fig. 2e). The median mean dose given to the ipsilateral optic nerve was higher with VMAT than with DCA-IMRT, although the differences were clearly below the clinical threshold (28 Gy). The median dose for DCA-IMRT was 7.3 Gy (0.4 Gy–22.2 Gy) and 13.4 Gy (8.2 Gy–17.4 Gy) for VMAT ($p < 0.01$).

The beam-on time for DCA-IMRT was 3.2 (± 0.4) min, and 2.9 (± 0.25) min. for VMAT The treatment session duration was 30.1 (± 11.8) min for DCA-IMRT. Treatment with VMAT was implementable, a time slot of 30 min would be appropriate, if to be scheduled.

4. Discussion

Multi-leaf collimator-based stereotactic radiotherapy has been a standard for many years for treating OM [1]. We currently offer patients stereotactic radiosurgery if brachytherapy with ^{106}Ruthenium eye applicators is not feasible or might result in suboptimal tumor dose coverage [16]. DCA-IMRT uses dynamic conformal arcs to supply steep dose gradients between the tumor and normal tissue and need not many monitor units; IMRT is used to homogenize the dose distribution in the planning target volume and reduce dose to neighbouring organs. In the case of photon beam therapy for eye tumors, both characteristics of dose distributions are needed, because some of the ipsilateral organs at risk are located in close proximity or even overlapping the planning target volume. In the present series, VMAT was inferior to DCA-IMRT. Even after optimization with automated planning, dose delivery was comparable to the target structure, but not for the OARs. In general, automated planning is efficient and delivers superior plans than operator-dependant planning [12,17].

Regarding the clinical utility of DCA-IMRT and VMAT, both techniques despite some physical differences are adequate for treating patients for OM. The dose exceeding 107% in the PTV was avoided with DCA-IMRT, compared to seven patients replanned with VMAT. However, the $V_{(PTV)}$ that received more than 107% was only 0.3% which corresponded approximately to a volume < 0.01 ccm, and conformity with both DCA-IMRT and VMAT were similar. A potentially clinical relevant difference was observed for the ipsilateral lens and cornea. Cataract formation and the risk of keratitis should likely to be avoided without compromises on the conformity. However, the clinical need for optimization must be weighted against the efforts. Minor improvements might impact on toxicity, such as visual acuity [18,19]. A major advantage of DCA-IMRT is, that in contrast to most data from radiosurgery or SBRT, we can apply constraints according to ICRU Report 62 [20]. Dose prescription according to ICRU is comparable and ascertains reproducibility. There is little reason to abandon ICRU constraints if feasible.

The reason why DCA-IMRT provides high planning quality that is unmatched with VMAT relies in the steep gradient achieved with DCA-IMRT, with a dose fall-off of up to seven Gy within one millimetre [21]. Obviously, the pay-off for high conformity is the robustness of the plans obtained with HA (Fig. 3). Therefore, positioning and target visualization is crucial, if treating with DCA-IMRT. We are currently using ExacTrac®, which provides X-ray imaging in two oblique angels visualizing *peri*-lesional fiducial markers for 6D-fusion and correction. Images are taken before every field and a patient positioning is performed to minimize the intra-fraction target motion. Possible motion of the eye that could lead to a target under dosage are corrected. Indeed, a deviation of two mm of the target could results in a reduction up to thirteen per cent of the target volume $V_{95\%}$. Thus, although radiotherapy is non-invasive, surgery will remain necessary for positioning verification and correction of the anatomical surrogates to localize the tumor during treatment.

The current available quality of photons plans with DCA-IMRT and

the implementation of optimal beam geometry will likely challenge proton therapy in the future and reassessment of the optimal modality as function of clinical presentation seems justified [6,22,23].

DCA-IMRT is an optimal treatment technique for photon beam therapy of OM. As a result, we regularly achieved excellent homogeneity and conformity indices for the planning target volumes. We observed all dose preconditions comply with ICRU report 62. If two thirds of the therapeutic dose is given by means of dynamic conformal arcs, we obtain dose gradients, which are not feasible with either conformal arcs, IMRT or VMAT alone.

Conflict of interest statement

Jerome Krayenbühl, Lothar Krause, Mrkus Wösle and Dr. Ciernik have no conflict of interests.

Acknowledgment

Presented in parts at ESTRO 36, Vienna, Austria 5-9 May 2017: ExacTrac®-based Fractionated Radiosurgery (fSRS) of Choroidal Melanoma (CM) (7th May 2017).

References

[1] Georg D, Dieckmann K, Bogner J, Zehetmayer M, Potter R. Impact of a micro-multileaf collimator on stereotactic radiotherapy of uveal melanoma. Int J Radiat Oncol Biol Phys 2003;55:881–91.
[2] Dieckmann K, Georg D, Zehetmayer M, Bogner J, Georgopoulos M, Potter R. LINAC based stereotactic radiotherapy of uveal melanoma: 4 years clinical experience. Radiother Oncol 2003;67:199–206.
[3] Weber DC, Bogner J, Verwey J, Georg D, Dieckmann K, Escude L, et al. Proton beam radiotherapy versus fractionated stereotactic radiotherapy for uveal melanomas: A comparative study. Int J Radiat Oncol Biol Phys 2005;63:373–84.
[4] Hocht S, Stark R, Seiler F, Heufelder J, Bechrakis NE, Cordini D, et al. Proton or stereotactic photon irradiation for posterior uveal melanoma? A planning intercomparison. Strahlenther Onkol 2005;181:783–8.
[5] Muller K, Naus N, Nowak PJ, Schmitz PI, de Pan C, van Santen CA, et al. Fractionated stereotactic radiotherapy for uveal melanoma, late clinical results. Radiother Oncol 2012;102:219–24.
[6] Dunavoelgyi R, Zehetmayer M, Gleiss A, Geitzenauer W, Kircher K, Georg D, et al. Hypofractionated stereotactic photon radiotherapy of posteriorly located choroidal melanoma with five fractions at ten Gy–clinical results after six years of experience. Radiother Oncol 2013;108:342–7.
[7] Somani S, Sahgal A, Krema H, Heydarian M, McGowan H, Payne D, et al. Stereotactic radiotherapy in the treatment of juxtapapillary choroidal melanoma: 2-year follow-up. Can J Ophthalmol 2009;44:61–5.
[8] Miralbell R, Caro M, Weber DC, Elizalde J, Perez-Ochoa A, Villa S, et al. Stereotactic radiotherapy for ocular melanoma: initial experience using closed eyes for ocular target immobilization. Technol Cancer Res Treat 2007;6:413–7.
[9] Liu H, Li J, Pappas E, Andrews D, Evans J, Werner-Wasik M, et al. Dosimetric validation for an automatic brain metastases planning software using single-isocenter dynamic conformal arcsDosimetric validation for an automatic brain metastases planning software using single-isocenter dynamic conformal arcs. J Appl Clin Med Phys 2016;17:6320.
[10] Narayanasamy G, Stathakis S, Gutierrez AN, Pappas E, Crownover R, Floyd 2nd JR, et al. A systematic analysis of 2 monoisocentric techniques for the treatment of multiple brain metastases. Technol Cancer Res Treat 2016.
[11] Robar JL, Thomas C. HybridArc: a novel radiation therapy technique combining optimized dynamic arcs and intensity modulation. Med Dosim 2012;37:358–68.
[12] Fogliata A, Wang PM, Belosi F, Clivio A, Nicolini G, Vanetti E, et al. Assessment of a model based optimization engine for volumetric modulated arc therapy for patients with advanced hepatocellular cancer. Radiat Oncol 2014;9:236.
[13] Tol JP, Dahele M, Delaney AR, Slotman BJ, Verbakel WF. Can knowledge-based DVH predictions be used for automated, individualized quality assurance of radiotherapy treatment plans? Radiat Oncol 2015;10:234.
[14] Kataria T, Sharma K, Subramani V, Karrthick KP, Bisht SS. Homogeneity Index: an objective tool for assessment of conformal radiation treatments. J Med Phys 2012;37:207–13.
[15] Feuvret L, Noel G, Mazeron JJ, Bey P. Conformity index: a review. Int J Radiat Oncol Biol Phys 2006;64:333–42.
[16] Krema H, Heydarian M, Beiki-Ardakani A, Weisbrod D, Xu W, Laperriere NJ, et al. Dosimetric and late radiation toxicity comparison between iodine-125 brachytherapy and stereotactic radiation therapy for juxtapapillary choroidal melanoma. Int J Radiat Oncol Biol Phys 2013;86:510–5.
[17] Krayenbuehl J, Norton I, Studer G, Guckenberger M. Evaluation of an automated knowledge based treatment planning system for head and neck. Radiat Oncol 2015;10:226.
[18] Gigliotti CR, Modorati G, Di Nicola M, Fiorino C, Perna LA, Miserocchi E, et al. Predictors of radio-induced visual impairment after radiosurgery for uveal melanoma. Br J Ophthalmol 2017.
[19] Thariat J, Grange JD, Mosci C, Rosier L, Maschi C, Lanza F, et al. Visual outcomes of parapapillary uveal melanomas following proton beam therapy. Int J Radiat Oncol Biol Phys 2016;95:328–35.
[20] Stroom JC, Heijmen BJ. Geometrical uncertainties, radiotherapy planning margins, and the ICRU-62 report. Radiother Oncol 2002;64:75–83.
[21] Wösle M, Krause L, Sreenivasa S, Vordermark D, Ciernik IF. Stereotactic radiotherapy for choroidal melanomas by means of HybridArc™. Strahlenther Onkol 2018. (in press).
[22] Bensoussan E, Thariat J, Maschi C, Delas J, Schouver ED, Herault J, et al. Outcomes after proton beam therapy for large choroidal melanomas in 492 patients. Am J Ophthalmol 2016;165:78–87.
[23] Verma V, Mehta MP. Clinical outcomes of proton radiotherapy for uveal melanoma. Clin Oncol (R Coll Radiol) 2016;28:e17–27.